

Comparative uptakes and biodistributions of internalizing vs. noninternalizing copper-64 radioimmunoconjugates in cell and animal models of colon cancer

Jeffrey N. Bryan^a, Fang Jia^a, Huma Mohsin^b, Geethapriya Sivaguru^a, William H. Miller^c, Carolyn J. Anderson^{f,g}, Carolyn J. Henry^{a,d}, Michael R. Lewis^{a,c,e,*}

^aDepartment of Veterinary Medicine and Surgery, University of Missouri-Columbia, Columbia, MO 65211, USA

^bDepartment of Chemistry, University of Missouri-Columbia, Columbia, MO 65211, USA

^cNuclear Science and Engineering Institute, University of Missouri-Columbia, Columbia, MO 65211, USA

^dDepartment of Internal Medicine, University of Missouri-Columbia, Columbia, MO 65212, USA

^eDepartment of Radiology, University of Missouri-Columbia, Columbia, MO 65212, USA

^fMallinckrodt Institute of Radiology, Washington University School of Medicine, St. Louis, MO 63110, USA

^gDepartment of Molecular Biology and Pharmacology, Washington University School of Medicine, St. Louis, MO 63110, USA

Received 7 February 2005; received in revised form 19 April 2005; accepted 19 May 2005

Abstract

Copper-64-labeled monoclonal antibodies (mAbs) have previously demonstrated unexpectedly effective tumor control in rodent models of cancer at relatively low tumor-absorbed radiation doses. This property has been associated with delivery platforms resulting in cellular internalization. The purpose of the present studies was to evaluate the *in vitro* internalization and *in vivo* distribution of a two-antibody model of ⁶⁴Cu radioimmunotherapy (RIT) in the same cell and animal models of cancer. Biodistributions of an internalizing antibody, cBR96, and a noninternalizing antibody, cT84.66, labeled with ⁶⁴Cu, were obtained in nude mice bearing LS174T colon carcinoma xenografts from 15 min to 48 h. The ⁶⁴Cu-DOTA-cBR96 conjugate demonstrated rapid tumor uptake, reaching 20.2% ID/g at 3 h and peaking at 35.4% ID/g by 24 h. Tumor accumulation of ⁶⁴Cu-DOTA-cT84.66 was more gradual, 8.19% ID/g at 3 h and 43.8% ID/g by 24 h, but maximum uptake was not statistically different from ⁶⁴Cu-DOTA-cBR96. Mouse xenograft dosimetry was estimated to be 1128 rad/mCi (304.9 mGy/MBq) for ⁶⁴Cu-DOTA-cBR96 and 1409 rad/mCi (380.5 mGy/MBq) for ⁶⁴Cu-DOTA-cT84.66. In LS174T cells, internalized radioactivity increased by a factor of 3.8 over 4 h for ⁶⁴Cu-DOTA-cBR96, but remained unchanged ⁶⁴Cu-DOTA-cT84.66. When normalized to uptake at 1 h, cellular efflux of ⁶⁴Cu was essentially identical for both mAbs. The biodistributions and tumor dosimetry of these internalizing and noninternalizing radiolabeled mAbs were sufficiently similar for direct comparison of the therapeutic efficacies of low doses of ⁶⁴Cu RIT agents in the same animal model of cancer.

© 2005 Elsevier Inc. All rights reserved.

Keywords: Copper-64; Radioimmunotherapy; Lewis^y; Carcinoembryonic antigen; LS174T; Cellular internalization

1. Introduction

Radiolabeled monoclonal antibodies (mAbs) have shown great promise for radioimmunotherapy (RIT) of cancer. Radioimmunotherapy has shown considerable efficacy against B-cell non-Hodgkin's lymphoma (NHL). However,

RIT of solid tumors has been far less effective in producing lasting remissions or tumor control. The slow plasma clearance properties of radiolabeled mAbs result in prolonged exposure of the bone marrow to ionizing radiation, often resulting in dose-limiting toxicity before therapeutic efficacy can be achieved. Further advancements in RIT may require the use of new radionuclides having emission characteristics that are more appropriate for solid tumor therapy.

Copper-64 is a cyclotron-produced radionuclide with an intermediate half-life ($T_{1/2}=12.7$ h) that decays by both β^+ (655 keV, 17.4%) and β^- (573 keV, 39.0%) emission,

* Corresponding author. Department of Veterinary Medicine and Surgery, College of Veterinary Medicine, University of Missouri-Columbia, Columbia, 379 E. Campus Drive, MO 65211, USA. Tel.: +1 573 814 6000x3703; fax: +1 573 814 6551.

E-mail address: lewismic@missouri.edu (M.R. Lewis).

making it suitable for labeling mAbs for positron emission tomography (PET) imaging and RIT of cancer. This radionuclide offers potential advantages for solid tumors over ^{131}I and ^{90}Y , used in clinical therapy of NHL. Iodinated mAbs can undergo dehalogenation, resulting in significant thyroid accumulation and clinical hypothyroidism [1]. Yttrium-90 emits no photon, requiring the surrogate imaging label ^{111}In to trace the therapeutic mAb. The 11-mm path length of the 2.27-MeV β^- of ^{90}Y increases potential bone marrow toxicity, limiting the total dose that can be delivered. This toxicity can be exacerbated by unstable chelation, as yttrium has high affinity for bone [2]. Several experiments in xenograft-bearing rodent models have demonstrated remarkable tumor cytotoxicity of internalizing ^{64}Cu radio-pharmaceuticals, at tumor-absorbed doses much lower than traditionally administered.

Connett et al. [3] reported 82% complete tumor regressions with histopathologic cure in Golden Syrian hamsters bearing 200-mg GW39 xenografts treated with ^{64}Cu -labeled anticolo-rectal carcinoma mAb 1A3, at a tumor-absorbed dose of only 586 rad (5860 mGy). The somatostatin analogue ^{64}Cu -TETA-Tyr³-octreotate also produced complete, but temporary, tumor remissions at low tumor-absorbed dose in the highly aggressive CA20948 rat pancreatic tumor model [4]. In vivo distribution studies of ^{64}Cu -TETA-octreotide demonstrated transchelation of ^{64}Cu to superoxide dismutase (SOD) in the liver of rats [5]. Further experiments to define subcellular localization of the ^{64}Cu from ^{64}Cu -TETA-octreotide revealed that the radio-metal accumulated in the nucleus (19.5%) and mitochondria (21.1%) of AR42J rat pancreatic tumor cells in vitro over a 24-h period [6]. There was no evidence that the somatostatin analogue itself had accumulated in these locations, lending further support to the likelihood that ^{64}Cu transchelates to copper cofactor enzymes, metalloproteins and copper-handling chaperones. These observations led us to hypothesize that ^{64}Cu -labeled internalizing delivery platforms cause cell death by mechanisms of copper-related DNA damage, mitochondrial destruction and disruption of critical intracellular constituents or processes. However, no study to date has compared internalizing and noninternalizing ^{64}Cu -labeled mAbs in an experimental RIT trial, in order to determine whether internalization is the single critical step in this enhanced cytotoxicity.

We previously reported the development and preliminary characterization of a two-antibody model for comparison of ^{64}Cu RIT [7]. The first mAb, cBR96, recognizes the Lewis^y ceramide variant reported to be present in multiple human and veterinary carcinomas [8,9]. Indirect evidence that this antibody is rapidly internalized after binding was provided by the fact that ricin A-chain and doxorubicin conjugates of the intact mAb and a single-chain derivative were cytotoxic in vitro [9,10]. The second mAb, cT84.66 [11], recognizes carcinoembryonic antigen (CEA), also present on numerous human carcinomas [12] and reported in veterinary hepatocellular carcinomas, rete testis mucinous adenocarcinomas

and choroid plexus carcinomas [13–15]. Indirect evidence that this antibody is not internalized after binding was demonstrated by the fact that a doxorubicin conjugate showed no cytotoxicity (Shively, J.E., personal communication). The LS174T nude mouse model was selected for evaluation of these radioimmunoconjugates, because it expresses both Lewis^y and CEA.

The purpose of the present studies was to characterize the internalization properties of ^{64}Cu -DOTA-cBR96 and ^{64}Cu -DOTA-cT84.66 in vitro, obtain comprehensive in vivo distributions of both conjugates, and calculate mouse xenograft dosimetry in preparation for preclinical therapy studies. Although previous studies suggest that cBR96 is rapidly internalized and cT84.66 is not, internalization and retention of ^{64}Cu conjugated to these mAbs has not been measured quantitatively in tumor cells. The results of these studies will allow design of a RIT study to compare the tumoricidal properties of the internalizing vs. the non-internalizing ^{64}Cu -labeled mAbs directly at relatively low, normalized tumor-absorbed doses.

2. Materials and methods

2.1. Monoclonal antibodies and labeling

The methods used to prepare the conjugates and perform quality-control evaluation have been described previously [7]. Copper-64 was produced on a biomedical cyclotron at Washington University School of Medicine by previously published methods [16]. Conjugates were labeled with ^{64}Cu at a specific activity of 10 $\mu\text{Ci}/\mu\text{g}$ [17]. Specific activity of labeling was determined prior to purification, and radiochemical purity was determined after purification, by SE-HPLC, using a Waters Delta 600 (Waters, Milford, MA) chromatograph equipped with a manual Rheodyne injector, a Waters 2487 dual wavelength UV detector, a Packard 500TR Flow Scintillation Analyzer (Packard, Downers Grove, IL) equipped with a GAMMA-C flow cell for ^{64}Cu , a Waters busSAT/IN analog–digital interface, and the Waters Millennium 32 software package. A Phenomenex BioSep-SEC-S 3000 (Phenomenex, Torrance, CA) column (7.8×300 mm, 5 μm , 290 Å), an isocratic mobile phase of 100 mM $\text{NaH}_2\text{PO}_4/0.05\%$ NaN_3 , pH 6.8 and a flow rate of 1.0 ml/min were used.

2.2. Animal model

The biodistribution studies were conducted in compliance with a protocol approved by the Animal Care and Use Committee of the University of Missouri-Columbia Animal Care Quality Assurance Office. Outbred female nu/nu mice (4–6 weeks of age) were obtained from Harlan Sprague Dawley (Indianapolis, IN). Mice were injected subcutaneously with 0.15 ml of Hank's Balanced Salt Solution containing 2×10^6 LS174T (The American Type Culture Collection, Manassas, VA) human colonic adenocarcinoma cells in the right prefemoral region via a 23-gauge needle.

Prior to radioimmunoconjugate administration, tumors were allowed to grow for 14 days to a mean weight of 189 mg.

2.3. Biodistribution studies

Seven groups of mice ($n=5$) bearing LS174T human colon cancer xenografts were injected intravenously via the tail vein with 10 μCi of either radiolabeled mAb. Groups were sacrificed at time points of 15 min, 1 h, 3 h, 6 h, 18 h, 24 h and 48 h postinjection. The following tissues were collected, drained of blood, weighed and counted in a Wallace 1480 Wizard 3" automated gamma counter (Perkin Elmer Life Sciences, Gaithersburg, MD): blood, lungs, liver, spleen, kidneys, urinary bladder, muscle, fat, heart, bone, uterus, ovaries, stomach, small intestine, large intestine, tumor, cranial carcass and caudal carcass. Each sample was counted with a 1% standard of the injected dose and an empty vial, such that background- and decay-corrected values were calculated as percent injected dose per gram of tissue (% ID/g) and percent injected dose per organ (% ID/organ).

2.4. Tumor dosimetry

Mouse xenograft absorbed doses were calculated as described previously [18,19] using a modification of the method of Hui et al. [20], which is based on the dimensions and masses of organs in a nude mouse of approximately 25 g body weight. All organs were modeled as ellipsoids, with the exception of bone and bone marrow. Whole femur was selected to represent the bone and bone marrow, which were modeled as concentric cylinders. Radioactivity was assumed to be uniformly distributed within each of the organs, the carcass and the tumor. Self-organ tumor-absorbed radiation energy was determined as the amount of absorbed energy remaining in the tumor per radioactive decay. Cross-organ tumor-absorbed radiation energy was determined using the approximation that the energy of beta particles that escaped the source organ was deposited in adjacent organs [20]. The ratios of energy deposited in the tumor from adjacent organs were assumed to be approximately proportional to the ratios of the surface areas that overlapped with the tumor. To better simulate the geometry of a flank xenograft, it was assumed that the tumor was a sphere, with half the volume in contact with the remainder of body and half, covered with 0.5 mm of skin, protruding above the surface.

The Monte Carlo radiation transport code MCNP-4C [21] was used to obtain absorbed fractions for monoenergetic β^- and β^+ particles. MCNP-4C was run in photon electron mode, in order to track both beta particles and bremsstrahlung radiation produced by the particles. To calculate absorbed fractions for the polyenergetic β^- and β^+ spectra of ^{64}Cu , absorbed fractions were first determined at 51 energies from 0.025 to 2.5 MeV. Beta spectra were then calculated using the NUCDECAY code [22], and these monoenergetic responses were numerically integrated over the ^{64}Cu spectra. An S value was calculated for an average tumor weight of 200 mg, assuming radioactivity to be uniformly distributed within a sphere of unit density. This approach assumes that tumors of

similar size in different animals have similar uptake characteristics, and the resulting absorbed dose is an average of that absorbed by each tumor.

2.5. Cell uptake and internalization studies

The methods for cell uptake and internalization were based on previously described techniques [23]. Six aliquots of 2×10^6 LS174T cells/ml, suspended in 15 ml of serum-free Eagle Minimum Essential Medium containing 5% CO_2 (Invitrogen, Carlsbad, CA), were incubated in an orbital shaking water bath at 37 °C. To each was added 0.2 $\mu\text{Ci}/\text{ml}$ of either ^{64}Cu -labeled DOTA-cBR96 or DOTA-cT84.66 (three vials each). After 1 min, 5 min, 15 min, 30 min, 1 h, 2 h and 4 h of incubation, 200- μL aliquots were removed and centrifuged at 10000 rpm for 1 min, after which the cell pellets and supernatants were separated. Using modifications of a previously described procedure [24], cells were resuspended in 500 μL of medium containing 0.2 U of glycosylphosphatidylinositol (GPI)-specific phospholipase C (Sigma, St. Louis, MO) for 90 min at 37 °C. These suspensions were centrifuged again, to separate the supernatants and cell pellets, which were treated with 1 ml of cold 0.5 M NaCl/0.1 M acetic acid to remove any additional surface-bound radioactivity. Radioactivity in each sample (supernatant, low pH fraction, phospholipase C fraction and cell pellet) was counted in the gamma counter. Internalization was calculated by dividing the pellet-associated radioactivity by the total radioactivity. Cell viability, as determined by trypan blue exclusion and hemacytometry, was >90% after 4 h of incubation.

2.6. Cell efflux studies

Six 5-ml suspensions of 2×10^6 LS174T cells/ml were incubated with either ^{64}Cu -DOTA-cBR96 or ^{64}Cu -DOTA-cT84.66, as described above for the uptake and internalization studies, for 1 h. The supernatant was removed, and the cells were washed with fresh medium and resuspended in the original volume. After 1 min, 5 min, 15 min, 30 min, 1 h, 2 h and 4 h following resuspension in fresh medium, 200- μL aliquots were removed and centrifuged at 10000 rpm for 1 min. Cell pellets and supernatants were separated and counted for each time point. Efflux was calculated by dividing the radioactivity in the cell pellet by the total radioactivity. Efflux values were then normalized to the cell uptake of each ^{64}Cu -labeled mAb at 1 h. Following the 4-h efflux period, cell viability was measured by trypan blue exclusion and hemacytometry and found to be >90%.

2.7. Statistical analysis

Biodistributions of tissue radioactivity, in % ID/g at each time point, were evaluated using a one-way analysis of variance (ANOVA). If a difference among groups was detected, a Tukey's test was performed. If groups failed an equal variance test, an ANOVA on ranks was performed with a subsequent Dunn's test if a difference was detected. Differences were considered significant at the 95% confidence level

Table 1
Biodistributions ($n=5$) of ^{64}Cu -DOTA-cBR96 in nude mice bearing LS174T tumors expressed in % ID/g \pm S.E.M.

Tissue	15 min	3 h	6 h	18 h	24 h	48 h
Blood	66.9 \pm 3.59	27.0 \pm 2.69	26.5 \pm 1.58	21.6 \pm 1.47	16.0 \pm 3.32	12.0 \pm 1.70
Lung	25.0 \pm 1.67	10.2 \pm 0.60	8.88 \pm 0.68	8.17 \pm 1.45	5.81 \pm 0.48	5.79 \pm 0.81
Liver	16.0 \pm 2.19	12.9 \pm 1.76	9.36 \pm 0.99	6.55 \pm 0.58	8.54 \pm 2.63	6.54 \pm 0.95
Spleen	11.7 \pm 0.68	10.5 \pm 1.40	5.48 \pm 0.88	5.19 \pm 0.70	9.05 \pm 3.58	4.21 \pm 0.60
Kidney	13.1 \pm 0.78	10.8 \pm 0.90	9.04 \pm 0.45	5.43 \pm 0.78	4.47 \pm 1.04	4.86 \pm 0.60
Bladder	1.45 \pm 0.17	2.41 \pm 0.37	3.25 \pm 0.40	3.86 \pm 0.45	6.05 \pm 1.10	3.93 \pm 0.80
Muscle	0.65 \pm 0.13	1.05 \pm 0.12	1.61 \pm 0.11	2.10 \pm 0.38	1.76 \pm 0.34	1.27 \pm 0.23
Fat	1.78 \pm 0.46	1.70 \pm 0.46	4.27 \pm 0.40	2.09 \pm 0.22	2.28 \pm 0.42	1.62 \pm 0.14
Heart	10.8 \pm 1.14	8.94 \pm 0.69	7.47 \pm 0.17	4.37 \pm 0.51	5.00 \pm 0.44	3.52 \pm 0.53
Bone	5.17 \pm 0.25	4.83 \pm 0.74	3.75 \pm 0.56	3.58 \pm 0.39	4.50 \pm 1.21	1.80 \pm 0.23
Uterus	2.97 \pm 0.58	4.43 \pm 0.98	6.56 \pm 1.24	10.4 \pm 0.90	13.2 \pm 1.45	9.24 \pm 1.17
Stomach	0.92 \pm 0.30	1.98 \pm 0.08	2.98 \pm 0.66	2.14 \pm 0.12	3.11 \pm 0.19	1.63 \pm 0.36
Small intestine	2.60 \pm 0.33	6.17 \pm 0.76	6.13 \pm 1.19	5.04 \pm 0.73	10.4 \pm 1.61	4.25 \pm 0.72
Large intestine	1.16 \pm 0.12	1.98 \pm 0.26	3.58 \pm 0.28	4.23 \pm 0.54	5.27 \pm 0.31	3.90 \pm 0.79
Tumor	6.43 \pm 0.91	20.2 \pm 0.56	24.2 \pm 1.92	26.4 \pm 1.96	35.4 \pm 4.46	33.2 \pm 3.17

($P<.05$). For the biodistribution data in which multiple dependent categories were examined, a Bonferroni adjustment was performed, in which the confidence interval is divided by the number of categorical variables, in this case dividing 0.05 by 16. This was necessary to account for the evaluation of multiple dependent variables that are interrelated. The level of significance was then set at $P\leq.003$. All analyses were performed using a commercial statistical software package (SPSS, Chicago, IL).

3. Results

3.1. Biodistributions

The biodistributions of ^{64}Cu -labeled DOTA-cBR96 and DOTA-cT84.66 are presented in Tables 1 and 2, respectively. The in vivo distributions of the two conjugates were very similar at all time points. Blood clearance, tumor uptake and clearance organ activity were comparable for both mAbs. Statistically significant differences were detected at only a few time points in 8 of 16 tissues. Tumor accumulation of ^{64}Cu -DOTA-cBR96 was significantly more

rapid, reaching 20.2% ID/g at 3 h compared to 8.12% ID/g for ^{64}Cu -DOTA-cT84.66 ($P<.002$). The ^{64}Cu -DOTA-cT84.66 conjugate demonstrated higher reticuloendothelial clearance. For example, the liver uptake of ^{64}Cu -DOTA-cT84.66 was significantly higher at 18 h, rising to 17.1% ID/g compared to 6.55% ID/g for ^{64}Cu -DOTA-cBR96 ($P<.001$). Similarly, the spleen uptake of ^{64}Cu -DOTA-cT84.66 was 27.4% ID/g at 18 h and 10.6% ID/g at 48 h, significantly higher than 5.19 and 4.01% ID/g for ^{64}Cu -DOTA-cBR96 at the same time points ($P\leq.001$, .003, respectively). The ^{64}Cu -DOTA-cBR96 conjugate demonstrated slower blood clearance with increased activity at 15 min, 6 h and 18 h ($P=.002$, .002 and $<.001$, respectively). This mAb also exhibited significantly higher kidney uptake, reaching 10.8% ID/g and 9.04% ID/g at 3 and 6 h vs. 6.22% ID/g and 5.56% ID/g for ^{64}Cu -DOTA-cT84.66 ($P=.002$, $<.001$, respectively).

3.2. Tumor dosimetry

The general Monte Carlo N-Particle Transport Code MCNP-4C was used to estimate mouse xenograft dosimetry

Table 2
Biodistributions ($n=5$) of ^{64}Cu -DOTA-cT84.66 in nude mice bearing LS174T tumors expressed in % ID/g \pm S.E.M.

Tissue	15 min	3 h	6 h	18 h	24 h	48 h
Blood	34.9 \pm 3.64	25.2 \pm 2.69	13.9 \pm 0.95	6.17 \pm 1.83	12.7 \pm 4.48	3.63 \pm 1.05
Lung	14.6 \pm 1.47	9.50 \pm 0.58	7.88 \pm 1.28	4.38 \pm 0.45	9.09 \pm 0.86	4.08 \pm 0.32
Liver	12.1 \pm 1.55	11.7 \pm 1.14	15.9 \pm 1.37	17.1 \pm 1.02	12.4 \pm 0.77	15.6 \pm 1.76
Spleen	10.6 \pm 1.72	6.92 \pm 0.77	16.4 \pm 1.79	27.4 \pm 1.75	6.84 \pm 0.38	10.6 \pm 1.20
Kidney	6.83 \pm 0.88	6.22 \pm 0.48	5.56 \pm 0.33	4.21 \pm 0.27	4.44 \pm 0.51	3.25 \pm 0.20
Bladder	1.52 \pm 0.26	2.51 \pm 0.50	2.93 \pm 0.47	2.96 \pm 0.32	5.82 \pm 0.56	2.62 \pm 0.41
Muscle	0.96 \pm 0.11	1.20 \pm 0.13	1.38 \pm 0.15	0.92 \pm 0.07	1.48 \pm 0.15	0.85 \pm 0.06
Fat	3.67 \pm 0.70	2.41 \pm 0.22	2.32 \pm 0.34	0.83 \pm 0.10	2.16 \pm 0.13	1.25 \pm 0.33
Heart	7.88 \pm 0.82	7.47 \pm 0.53	5.67 \pm 0.40	3.48 \pm 0.54	4.98 \pm 0.14	2.73 \pm 0.08
Bone	4.45 \pm 0.36	3.18 \pm 0.20	6.33 \pm 0.92	8.39 \pm 0.36	2.50 \pm 0.14	2.20 \pm 0.14
Uterus	2.32 \pm 0.63	4.94 \pm 0.41	7.14 \pm 0.71	5.16 \pm 1.17	12.5 \pm 1.12	9.10 \pm 1.83
Ovaries	6.74 \pm 0.96	5.22 \pm 0.70	5.83 \pm 0.31	6.25 \pm 1.41	5.70 \pm 0.67	2.70 \pm 0.30
Stomach	0.56 \pm 0.26	1.86 \pm 0.20	2.06 \pm 0.19	1.24 \pm 0.20	1.63 \pm 0.34	1.05 \pm 0.08
Small Intestine	2.01 \pm 0.24	3.39 \pm 0.50	4.87 \pm 0.59	5.16 \pm 0.09	3.29 \pm 0.96	3.35 \pm 0.58
Large Intestine	0.77 \pm 0.09	1.74 \pm 0.05	2.28 \pm 0.05	2.68 \pm 0.27	2.30 \pm 0.27	2.93 \pm 0.06
Tumor	2.94 \pm 0.31	8.19 \pm 0.33	18.8 \pm 1.92	16.6 \pm 1.72	43.8 \pm 5.63	32.5 \pm 3.91

for ^{64}Cu -labeled DOTA-cBR96 and DOTA-cT84.66. The tumor-absorbed dose for a mean tumor mass of 200 mg was calculated to be 1128 rad/mCi (304.9 mGy/MBq) for ^{64}Cu -DOTA-cBR96 and 1408 rad/mCi (380.5 mGy/MBq) for ^{64}Cu -DOTA-cT84.66. The results of these calculations indicated that self-dose contributed to 99.8–99.9% of the tumor-absorbed dose for each ^{64}Cu -labeled mAb, with the remaining 0.1–0.2% representing cross-organ doses from blood, muscle, fat and remainder of the body.

3.3. Cell uptake and internalization

Maximal uptake of ^{64}Cu -DOTA-cBR96 in LS174T cells occurred at 30 min, reaching 5.18% of the total radioactivity added to the suspension. At 1 h, cell uptake of the cBR96 conjugate was similar at 4.59% of the total ^{64}Cu , and at 4 h, cell uptake was 3.65%. In contrast, maximal uptake for ^{64}Cu -DOTA-cT84.66 apparently was not reached after 4 h of incubation, as it continued to rise at that time to 41.6% of total radioactivity from a value of 23.1% at 1 h. Because of the difference in uptake profiles between the two ^{64}Cu -labeled mAbs, internalized radioactivity was calculated as the percentage of cell-associated radioactivity, normalized to the 1-min time point (Fig. 1). The cBR96 conjugate displayed substantial internalization of ^{64}Cu , doubling by 15 min and tripling by 4 h of incubation, following removal of surface-bound radioactivity with GPI-specific phospholipase C and a high-salt, low-pH buffer. After cleavage of CEA-bound ^{64}Cu -DOTA-cT84.66 with GPI-specific phospholipase C and washing with a high-salt, low-pH solution, the percentage of internalized radioactivity from ^{64}Cu -DOTA-cT84.66 remained essentially static over 4 h of incubation.

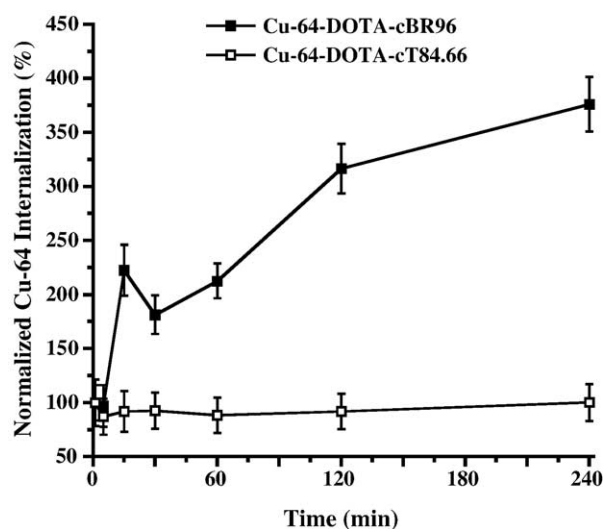


Fig. 1. Internalization of ^{64}Cu from DOTA-cBR96 and DOTA-cT84.66 in LS174T cells in suspension at 37°C and 5% CO_2 . Values (mean \pm S.D.) are expressed as the percentages of cell-associated radioactivity normalized to the cell uptakes at 1 min.

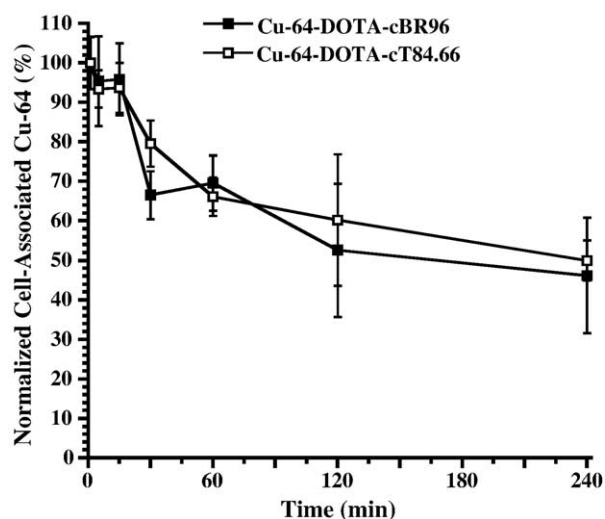


Fig. 2. Efflux of ^{64}Cu from LS174T cells in suspension, following 1-h incubations with ^{64}Cu -labeled DOTA-cBR96 and DOTA-cT84.66 at 37°C and 5% CO_2 . Values (mean \pm S.D.) are expressed as percentages normalized to the cell uptakes at 1 h.

3.4. Cell efflux

Cellular efflux of ^{64}Cu , following a 1-h “pulse-chase” incubation, is presented for each mAb in Fig. 2. Despite the differences in cell-uptake kinetics between the two mAbs, the data were normalized to cell-associated radioactivity after 1 h of incubation, for purposes of maintaining cell viability over the course of the subsequent 4-h efflux study. Over the 4-h period, 46.2% of the activity remained associated with the cell pellet following uptake of ^{64}Cu -DOTA-cBR96. Similarly, 50.0% of the activity remained associated with the cell pellet after incubation with ^{64}Cu -DOTA-cT84.66. Efflux curves were quantitatively similar for both mAbs, with the percentage of ^{64}Cu retained nearly identical at all time points.

4. Discussion

The biodistributions of ^{64}Cu -labeled DOTA-cBR96 and DOTA-cT84.66 were sufficiently similar for purposes of comparison in RIT studies. However, some notable differences in blood and reticuloendothelial clearance, as well as tumor uptake, of the ^{64}Cu -labeled antibodies were observed. In a study of humans receiving ^{67}Cu -labeled monoclonal antibodies, low-level transchelation to the plasma protein ceruloplasmin was shown to occur in all patients [25]. Binding to this major serum protein resulted in alteration of the blood-activity disappearance curve. Similarly, in this study, accumulation of ceruloplasmin-bound ^{64}Cu from DOTA-cBR96 could account for a portion of increased blood levels and liver uptake. The most likely explanation for the faster blood clearance and higher liver uptake of ^{64}Cu -DOTA-cT84.66 is that CEA is shed continuously into circulation by tumor cells and subsequently cleared by

receptor-mediated endocytosis in the liver [26]. In vivo experiments in rats demonstrated that ^{64}Cu was incorporated into superoxide dismutase (SOD) in the hepatocytes of rats administered ^{64}Cu -labeled somatostatin analogues [5]. In the case of ^{64}Cu -DOTA-cT84.66, increased transchelation of ^{64}Cu to intracytoplasmic proteins such as SOD could enhance hepatic accumulation compared to ^{64}Cu -DOTA-cBR96.

The more rapid blood clearance of ^{64}Cu -DOTA-cT84.66, as compared to ^{64}Cu -DOTA-cBR96, could also be explained by enhanced hepatic uptake. Circulating CEA in tumor-bearing mice could serve as an immediate sink for the mAb and result in more rapid localization of immune complexes to the liver. As the binding affinity of cT84.66 for CEA is extremely high ($1.16 \times 10^{11} \text{ M}^{-1}$) [27], hepatic uptake may occur very rapidly after injection. In the present studies, liver radioactivity increased more rapidly for ^{64}Cu -DOTA-cT84.66 than for ^{64}Cu -DOTA-cBR96 at early time points. Although this is a notable trend, after application of the Bonferroni adjustment, it did not reach statistical significance at any time point except 18 h.

The observation of decreased blood clearance also raises the question of whether ^{64}Cu -DOTA-cBR96 exhibits binding to the vascular endothelium in mice. We have obtained preliminary evidence of this property by high-resolution PET imaging in LS174T-bearing nude mice, which will be reported in the future. While the cBR96 conjugate exhibited a lower tumor-to-blood ratio, the cT84.66 conjugate showed a lower tumor-to-liver ratio. These results suggest that potential bone marrow toxicity resulting from blood irradiation by the anti-Lewis^y mAb may be offset by cross-organ bremsstrahlung irradiation from liver accumulation of the anti-CEA mAb. Both of these factors are important considerations for clinical RIT. Differences in blood, liver and spleen uptakes between the two ^{64}Cu -labeled mAbs may be important contributors to dose-limiting toxicity, and these differences have also been confirmed by high-resolution PET imaging.

Tumor uptake increased earlier for ^{64}Cu -DOTA-cBR96 than for ^{64}Cu -DOTA-cT84.66. A possible explanation for the earlier tumor uptake of ^{64}Cu -labeled cBR96 is the lack of circulating antigen. As Lewis^y is not shed from tumors, there is no antigen in the blood for ^{64}Cu -DOTA-cBR96 to bind, potentially allowing for faster accumulation in the tumor. An alternative possibility is that the internalization of bound ^{64}Cu -labeled cBR96 results in recycling of the Lewis^y antigen, creating a cell surface “target” gradient that drives more rapid tumor uptake. These possible mechanisms may contribute to more favorable delivery of an intermediate-lived radionuclide like ^{64}Cu , as it localizes more radioactivity to the tumor before it has decayed. However, earlier tumor uptake of ^{64}Cu -DOTA-cBR96 was not entirely unexpected, given that the affinity constant of cBR96 for the Lewis^y antigen is 10^7 M^{-1} [9], four orders of magnitude below the affinity constant of cT84.66. The higher affinity of cT84.66 may contribute to an antigen “binding site barrier” that decreases tumor penetration. PET imaging showed that

xenograft uptake was heterogeneous for both mAbs, but ^{64}Cu -DOTA-cT84.66 appeared to have greater accumulation in the vascular periphery of the tumor in LS174T-bearing mice. These results will be reported in the future.

While significantly greater tumor accumulation of ^{64}Cu occurred for cBR96 at 3 h, there were no significant differences in tumor uptake between the two mAbs at later time points. Moreover, the very similar tumor uptakes of this two-antibody model in LS174T-bearing nude mice resulted in comparable tumor-absorbed radiation doses. Despite differences in affinity, mechanisms of antigen-mediated uptake and initial rate of tumor accretion, the LS174T xenograft absorbed dose was only 20% lower for ^{64}Cu -DOTA-cBR96 than for ^{64}Cu -DOTA-cT84.66. This latter finding will enable us to test the hypothesis that cellular internalization is the single critical step for enhanced tumor cytotoxicity of ^{64}Cu , by performing RIT studies in the LS174T mouse model at normalized tumor-absorbed doses considered to be subtherapeutic.

In vitro experiments demonstrated the rapid LS174T cell uptake of both ^{64}Cu -DOTA-cBR96 and ^{64}Cu -DOTA-cT84.66. However, the much greater affinity constant of cT84.66 apparently allowed a far larger percentage of the ^{64}Cu -DOTA conjugate to associate with its cell surface antigen in vitro over the 4-h experimental period. This finding rendered direct comparison of in vitro uptake between the two mAbs likely to be of little value. However, by 1 h, cellular uptake of both ^{64}Cu -labeled mAbs was sufficient to allow normalized comparison of internalization and efflux.

Evidence of cellular internalization of mAb cBR96 was previously inferred from the in vitro cytotoxicity of the ricin A-chain BR96 conjugate [9]. Evidence for lack of internalization of cT84.66 was previously inferred from the lack of in vitro cytotoxicity of a doxorubicin conjugate (Shively, J.E., personal communication). Although these are indirect methods of evaluating internalization, they do not allow quantitative measurement of the percentage of antibody or cytotoxic payload internalized. The in vitro studies presented here quantified the percentage of ^{64}Cu internalized in LS174T cells when conjugated to cBR96, under conditions of antigen excess.

The internalization curve of ^{64}Cu -DOTA-cBR96 showed a clear upward trend, with more than a tripling of internalized radioactivity after 4 h. This observation confirmed the internalizing property of ^{64}Cu -DOTA-cBR96. The mAb cT84.66 would not be expected to internalize, binding to a GPI-linked cell surface glycoprotein. During the internalization studies, the relative proportion of cell-associated ^{64}Cu from DOTA-cT84.66 remained constant from the first time point to 4 h. This is most consistent with a constant proportion of GPI-specific phospholipase C cleavage of ^{64}Cu -DOTA-cT84.66–CEA complexes bound to the cell surface.

The in vitro cellular efflux of ^{64}Cu was essentially identical for the two mAbs. This was a surprising result, as internalization would be expected to cause residualization of the radioactivity within the cells, e.g., by transchelation to

intracellular proteins like SOD. The decline in cell-associated activity can be explained in several ways. First, ^{64}Cu -DOTA-cBR96 may dissociate from the Lewis^y antigen prior to internalization [9], depositing radioactivity back into the supernatant. Similarly, CEA is spontaneously shed from the cell surface and may release bound ^{64}Cu -DOTA-cT84.66 in the supernatant. Second, internalized, macrocyclic-bound ^{64}Cu has been demonstrated to transchelate to other copper-containing biomolecules [5]. This could lead to active efflux by membrane associated chaperones such as the copper transporter family (Ctr1), Cu^+ -ATPase, or even cMOAT [28–30]. As cT84.66 is not internalized, active efflux of ^{64}Cu would not be expected to occur.

Differences in tumor internalization and efflux between the two mAbs may have important implications for ^{64}Cu radiation dosimetry. Copper-64 decays by electron capture (1.68 MeV, 40.5%) emitting an average of 2 Auger/conversion electrons per decay. Therefore, substantial localization of ^{64}Cu within the nucleus [6] or in close proximity would be expected to enhance tumor cell killing, as would high uptake in mitochondria [6], potentially causing mitochondrial DNA damage and respiratory cell death. Conversely, accumulation of ^{64}Cu in lysosomes would be expected to lessen intracellular dosimetry by abrogating the biological damage of high linear energy transfer Auger/conversion electrons to nuclear and mitochondrial DNA. Yet when all emissions (β^- , β^+ , Auger/conversion electrons, X-rays, γ rays) are taken into account, internalizing ^{64}Cu -labeled radiopharmaceuticals have demonstrated remarkable therapeutic efficacy at tumor-absorbed doses far lower than generally considered tumoricidal [3,4,31].

The observed lack of residualization of ^{64}Cu from DOTA-cBR96 is disquieting, as it may represent loss of the enhanced cytotoxicity potentially attributable to intracellular ^{64}Cu . However, the biodistribution results obtained here appeared to show a “steady state” of ^{64}Cu uptake from the cBR96 mAb in the tumor at longer time points. A major efflux of ^{64}Cu from DOTA-cBR96 in the tumor did not appear to take place in vivo. Therefore, caution should be exercised in making direct comparisons between the in vitro internalization and efflux properties of these two mAbs and their in vivo behavior in tumor-bearing mice. Comparative RIT studies in LS174T-bearing nude mice, using ^{64}Cu -labeled cBR96 and cT84.66, are being performed to investigate whether a cellular efflux phenomenon has consequences in vivo. The results of these studies will be reported in the future.

5. Conclusions

The studies reported here confirm the suitability of this two-antibody model for direct comparison of ^{64}Cu RIT. Previous experiments in rodent models of cancer have demonstrated a remarkable ability of internalizing ^{64}Cu -labeled monoclonal antibodies and peptides to cause complete tumor remissions at tumor radiation absorbed

doses far below those generally considered to be therapeutic. Radioimmunotherapy studies of ^{64}Cu -DOTA-cBR96 and ^{64}Cu -DOTA-cT84.66 will compare the efficacies of these radioimmunoconjugates administered at relatively low and normalized tumor doses. The similar biodistributions and tumor dosimetry of this two-antibody model limit the variables in the study to the internalizing delivery of ^{64}Cu . This RIT experiment is designed to demonstrate whether internalization is the sole property of a delivery platform or a tumor cell target necessary to cause enhanced tumor cytotoxicity at doses of ^{64}Cu radiation traditionally considered to be subtherapeutic. Previous examination of its subcellular localization both in vitro [6] and in vivo [5] has suggested that ^{64}Cu dissociates from the bioconjugate chelate and localizes to intracellular compartments, potentially eliciting mechanisms of cytotoxicity in addition to classical ionizing radiation damage. The results of ^{64}Cu -labeled DOTA-cBR96 and DOTA-cT84.66 RIT studies will help to elucidate what internalizing and residualizing properties of ^{64}Cu radiotherapeutics hold promise for future preclinical and clinical applications.

Acknowledgments

This research was funded in part by the University of Missouri College of Veterinary Medicine Committee on Research. The production of ^{64}Cu at Washington University School of Medicine is supported by the NIH grant R24 CA86307 from the National Cancer Institute. The authors would like to thank Dr. Clay Siegall of Seattle Genetics for materials that made this research possible. The authors would also like to thank Drs. Jack Shively and Andrew Raubitschek of the City of Hope National Medical Center and Beckman Research Institute for providing DOTA-cT84.66, as well as Dr. Shively for helpful discussions. The authors acknowledge the support of the U.S. Department of Veterans Affairs, for providing resources and the use of facilities at the Harry S. Truman Memorial Veterans' Hospital in Columbia, MO.

References

- [1] Kaminski MS, Estes J, Zasadny KR, Francis IR, Ross CW, Tuck M, et al. Radioimmunotherapy with iodine (^{131}I) tositumomab for relapsed or refractory B-cell non-Hodgkin lymphoma: updated results and long-term follow-up of the University of Michigan experience. *Blood* 2000;96:1259–66.
- [2] Govindan SV, Shih LB, Goldenberg DM, Sharkey RM, Karacay H, Donnelly JE, et al. ^{90}Y -labeled complementarity-determining-region-grafted monoclonal antibodies for radioimmunotherapy: radio-labeling and animal biodistribution studies. *Bioconjug Chem* 1998; 9:773–82.
- [3] Connett JM, Anderson CJ, Guo LW, Schwarz SW, Zinn KR, Rogers BE, et al. Radioimmunotherapy with a ^{64}Cu -labeled monoclonal antibody: a comparison with ^{67}Cu . *Proc Natl Acad Sci U S A* 1996; 93:6814–8.
- [4] Lewis JS, Lewis MR, Cutler PD, Srinivasan A, Schmidt MA, Schwarz SW, et al. Radiotherapy and dosimetry of ^{64}Cu -TETA-Tyr³-octeotate

- in a somatostatin receptor-positive, tumor-bearing rat model. *Clin Cancer Res* 1999;5:3608–16.
- [5] Bass LA, Wang M, Welch MJ, Anderson CJ. In vivo transchelation of copper-64 from TETA-octreotide to superoxide dismutase in rat liver. *Bioconjug Chem* 2000;11:527–32.
- [6] Wang M, Caruano AL, Lewis MR, Meyer LA, VanderWaal RP, Anderson CJ. Subcellular localization of radiolabeled somatostatin analogues: implications for targeted radiotherapy of cancer. *Cancer Res* 2003;63:6864–9.
- [7] Bryan JN, Lewis MR, Henry CJ, Owen NK, Zhang J, Mohsin H, et al. Development of a two-antibody model for the evaluation of copper-64 radioimmunotherapy. *Vet Comp Oncol* 2004;2:82–90.
- [8] Henry CJ, Buss MS, Hellström I, Hellström KE, Brewer WG, Bryan JN, et al. Clinical evaluation of BR96 sFv-PE40 immunotoxin therapy in canine models of spontaneously occurring invasive carcinoma. *Clin Cancer Res* 2005;11:751–5.
- [9] Hellstrom I, Garrigues HJ, Garrigues U, Hellstrom KE. Highly tumor-reactive, internalizing, mouse monoclonal antibodies to Le(y)-related cell surface antigens. *Cancer Res* 1990;50:2183–90.
- [10] Muldoon LL, Neuwelt EA. BR96-DOX immunoconjugate targeting of chemotherapy in brain tumor models. *J Neurooncol* 2003;65:49–62.
- [11] Neumaier M, Shively L, Chen FS, Gaida FJ, Ilgen C, Paxton RJ, et al. Cloning of the genes for T84.66, an antibody that has a high specificity and affinity for carcinoembryonic antigen, and expression of chimeric human/mouse T84.66 genes in myeloma and Chinese hamster ovary cells. *Cancer Res* 1990;50:2128–34.
- [12] Shoukat D, Hannigan GE, Rak J, Kerbel RS. The extracellular environment and cancer. In: Tannock IF, Hill RP, editors. *The basic science of oncology*. New York: McGraw-Hill; 1998. p. 197–218.
- [13] Cantile C, Campani D, Menicagli M, Arispici M. Pathological and immunohistochemical studies of choroid plexus carcinoma of the dog. *J Comp Pathol* 2002;126:183–93.
- [14] Martin de las Mulas J, Gomez-Villamandos JC, Perez J, Mozos E, Estrado M, Mendez A. Immunohistochemical evaluation of canine primary liver carcinomas: distribution of alpha-fetoprotein, carcinoembryonic antigen, keratins and vimentin. *Res Vet Sci* 1995;59:124–7.
- [15] Radi ZA, Miller DL, Hines II ME. Rete testis mucinous adenocarcinoma in a dog. *Vet Pathol* 2004;41:75–8.
- [16] McCarthy DW, Shefer RE, Klinkowstein RE, Bass LA, Margeneau WH, Cutler CS, et al. Efficient production of high specific activity ⁶⁴Cu using a biomedical cyclotron. *Nucl Med Biol* 1997;24:35–43.
- [17] Lewis MR, Boswell CA, Laforest R, Buettner TL, Ye D, Connett JM, et al. Conjugation of monoclonal antibodies with TETA using activated esters: biological comparison of ⁶⁴Cu-TETA-1A3 with ⁶⁴Cu-BAT-2IT-1A3. *Cancer Biother Radiopharm* 2001;16:483–94.
- [18] Miller WH, Hartmann-Siantar C, Descalle M-A, Lehmann J, Lewis MR, Hoffman T, et al. Mouse organ absorbed dose fractions for beta emitters. *Trans Am Nucl Soc* 2003;89:689–92.
- [19] Miller WH, Hartmann-Siantar C, Fisher D, Descalle M-A, Daly T, Lehmann J, et al. Evaluation of beta absorbed fractions in a mouse model for ⁹⁰Y, ¹⁸⁸Re, ¹⁶⁶Ho, ¹⁴⁹Pm, ¹⁷⁷Lu and ⁶⁴Cu radioisotopes. *Cancer Biother Radiopharm* [in press].
- [20] Hui TE, Fisher D, Kuhn JA, Williams LE, Nourigat C, Badger CC, et al. A mouse model for calculating cross organ beta doses from yttrium-90-labeled immunoconjugates. *Cancer* 1994;73(Suppl):951–7.
- [21] Briesmeister JE. MCNP — A general Monte Carlo N-particle transport code, version 4C, report LA-13709-M. Los Alamos (NM): Los Alamos National Laboratory; 2000.
- [22] ORNL. NUCDECAY: nuclear decay data for radiation dosimetry calculations for ICRP and MIRD. RSICC DATA LIBRARY DLC-172. Oak Ridge (Tenn): Oak Ridge National Laboratories; 1995.
- [23] Smith CJ, Sieckman GL, Owen NK, Hayes DL, Mazuru DG, Kannan R, et al. Radiochemical investigations of gastrin-releasing peptide receptor-specific [^{99m}Tc(X)(CO)₃-Dpr-Ser-Ser-Ser-Gln-Trp-Ala-Val-Gly-His-Leu-Met-(NH₂)] in PC-3, tumor-bearing, rodent models: syntheses, radiolabeling, and in vitro/in vivo studies where Dpr=2,3-diaminopropionic acid and X=H₂O or P(CH₂OH)₃. *Cancer Res* 2003;63:4082–8.
- [24] Khan WN, Hammarström S. Biosynthesis of carcinoembryonic antigen (CEA) gene family members expressed in human tumor cell lines: evidence for cleavage of the glycosyl phosphatidyl inositol (GPI) anchor by GPI-PLC and GPI-PLD. *Biochem Int* 1991;25:723–31.
- [25] Mirick GR, O'Donnell RT, DeNardo SJ, Shen S, Meares CF, DeNardo GL. Transfer of copper from a chelated ⁶⁷Cu-antibody conjugate to ceruloplasmin in lymphoma patients. *Nucl Med Biol* 1999;26:841–5.
- [26] Bajenova O, Stolper E, Gapon S, Sundina N, Zimmer R, Thomas P. Surface expression of heterogeneous nuclear RNA binding protein M4 on Kupffer cell relates to its function as a carcinoembryonic antigen receptor. *Exp Cell Res* 2003;291:228–41.
- [27] Wong JYC, Chu DZ, Yamauchi DM, Williams LE, Liu A, Wilczynski S, et al. A phase I radioimmunotherapy trial evaluating ⁹⁰yttrium-labeled anti-carcinoembryonic antigen (CEA) chimeric T84.66 in patients with metastatic CEA-producing malignancies. *Clin Cancer Res* 2000;6:3855–63.
- [28] Mandal AK, Yang Y, Kertesz TM, Arguello JM. Identification of the transmembrane metal binding site in Cu⁺ transporting PIB-type ATPases. *J Biol Chem* 2004;279:54802–7.
- [29] Yoo J, Reichert DE, Kim J, Anderson CJ, Welch MJ. A potent Dubin-Johnson syndrome imaging agent: synthesis, biodistributions, and microPET imaging. *Mol Imaging* 2005;4:18–29.
- [30] Sharp PA. Ctrl1 and its role in body copper homeostasis. *Int J Biochem Cell Biol* 2003;35:288–91.
- [31] Connett JM, Buettner TL, Anderson CJ. Maximum tolerated dose and large tumor radioimmunotherapy studies of ⁶⁴Cu-labeled monoclonal antibody 1A3 in a colon cancer model. *Clin Cancer Res* 1999;5:3207s–12s.